Part II. The Solids Flow Properties

TE-YU CHEN
WALTER P. WALAWENDER
and
L. T. FAN

Department of Chemical Engineering
Kansas State University
Manhattan, Kansas 66506

The purpose of part II of this paper is to theoretically analyze and experimentally examine moving-bed solids flow in an inclined pipe connecting a fluidized bed and a solids storage vessel. The macroscopic momentum balance equation is simplified and applied to the present system. A friction factor correlation is developed. Based on the flow curves constructed, we found that the power law model is suitable for describing moving-bed solids flow.

SCOPE

In many fluidized bed operations, the transfer of solids between two fluidized beds is an indispensable process. Solids may be transferred in one of the three flow regimes: pneumatic conveying, fluidized bed, and moving bed. The present work is concerned with the last type.

Fluidized bed processes where solids are transferred as moving beds have been recently proposed (Bailie 1974, Kunii et al. 1974, Engler et al. 1975). These processes have been successful, both in the production of olefins from heavy oil and the gasification of organic slurries (Kunii et al. 1974), and in solids waste (Kunii et al. 1977). Despite these applications, studies of this phenomenon reported in the literature have been very few. Chari (1971) studied the horizontal transport of four types of relatively incompressible solids i.e., a batch of solid particles which show only a very small increase in the bulk density on tapping. Wilson et al. (1972) studied the flow of liquid media containing solid particles, and developed the so-called slip-model. Trees (1962) appears to be the first to report on solids flow in an inclined pipe connecting two fluidized beds. He conducted experiments with three angles of inclination and several pipe diameters and lengths. In addition, he examined the effect of pressure drop on the solids flow rate and empirically correlated the solids flow rate with these four variables.

Moving-bed flow in inclined pipes was also investigated by Kunii et al. (1974). In their work, two inclined pipes connected two fluidized beds to form a circulation system. They concluded that the friction in the pipes determines the solids circulation rate. In a similar circulation system, Chen et al. (1978) examined the influence of various operating parameters on the rate of solids transfer, including the fluidizing gas velocity, initial (packed-bed) height of the fluidized bed, location of the transfer line inlet, presence of internals, and the distributor design. The results were interpreted qualitatively, in terms of the difference between the bulk density in the transfer line and that in the fluidized bed.

Moving-bed solids flow in an inclined pipe can be satisfactorily described by the macroscopic momentum balance for heterogeneous flow systems provided that a proper friction factor is defined. The data of Trees (1962) show that the friction factor for solids is mainly a function of the solids flow rate and the pipe diameter (Chen et al. 1979).

The purpose of our work is to study moving-bed solids flow in an inclined pipe leading into a fluidized bed. Unlike the work of Trees (1962) where the major parameters were the pipe dimensions, the present work emphasizes the influence of the gas flow rate in the transfer line, the solids particle size, and the distributor design on the rate of solids flow.

CONCLUSIONS AND SIGNIFICANCE

The simplified momentum balance equation can be applied to the moving-bed solids flow through an inclined transfer line leading into a fluidized bed. An empirical friction factor correlation and flow curves, analogous to those in fluid flow, have been established from our experimental data.

The friction factor correlation has been expressed as a function of the variables examined here, namely, pipe diameter, mean particle diameter, gas flow rate in the pipe and solids velocity. The flow curves show that moving-bed solids can be well described by the power-law model. The power-law indices, viz., the "consistency" index and the "flow behavior" index, are found to be functions of the slip velocity—the relative velocity between gas and solids. The decrease in the consistency index with an increase in the slip velocity indicates that the bulk solids become less viscous as the slip velocity goes up. Since the flow-behavior index changes with variation of the slip velocity, the latter is seen to affect the degree of non-Newtonian behavior of the solids as well as the velocity profile in the pipe. The friction factor data agree well with predictions made by Metzner and Reed (1955).

Results of this work suggest that their generalized friction factor correlation (Metzner and Reed 1955) may be used for designing moving bed solids flow systems, although further investigations are necessary for this to be implemented.

ANALYSIS

According to Newton's laws of motion, the rate of change of the momentum of a system is equal to the rate of momentum influx through the external surface of the system plus the contributions of momentum influx due to external surface forces and external body forces exerting on the system. Thus we can write (Standart 1964):

$$\frac{d}{dt}\int_V \rho\,\overline{v}\,dV = -\oint_{A_e} \{\rho\,\overline{v}\,(\overline{v}-\overline{v}_e) + P\overline{\overline{U}} + \overline{\overline{\tau}}\} \cdot d\overline{A} + \Sigma\int_v \rho_i \overline{F}_i dV. \quad (1)$$

Present address for Chen is UOP Process Division, Drawer C, Riverside, IL 60546.
Address all correspondence to Walawender at Kansas State Univ.

001-1541-80-3088-0031-$00.85.

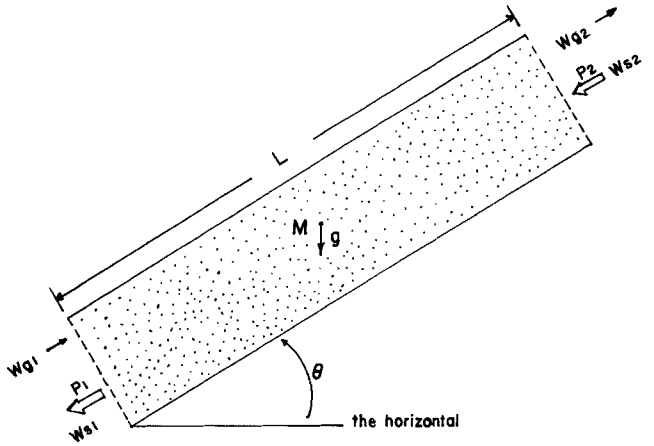

Figure 1. The transfer line section.

This balance can be applied to flow in the transfer line. The system under consideration is schematically presented in Figure 1. Equation (1) can be modified, under the assumptions that 1) the only external force is gravitational, 2) the flow is a steady-state, two-phase (gas-solids), one-dimensional, counter-current flow with no mass transfer through the pipe wall, 3) the pipe is straight and has a constant cross-sectional area, 4) the inertial terms can be neglected, and 5) the bulk solids density in the system is approximately constant. Equation (1) is simplified to (Chen et al. 1979):

$$\rho_b AL \sin\theta - A(P_1 - P_2) - F_{w\tau} = 0. \tag{2}$$

Note that $(P_1 - P_2)$ in Equation (2) is the pressure drop over the length of the transfer line. Other variables in the equation can be easily measured, except the friction loss term, $F_{w\tau}$. This can be determined from either the friction factor correlation or the flow curve equation.

Friction Factor

Although the wall friction contains contributions from both gas and solids, that from gas is negligible (Stemerding 1962). Therefore, analogous to the Fanning friction factor for the flow of fluid in a pipe (Bird et al. 1960), a friction factor for the solids flow can be defined by

$$f_b = \frac{\dfrac{D_t F_{w\tau}}{4AL}}{\dfrac{1}{2}\rho_b v_s^2} = \frac{\dfrac{D_t}{4}\left(\rho_b g \sin\theta - \dfrac{P_1 - P_2}{L}\right)}{\dfrac{1}{2}\rho_b v_s^2} \tag{3}$$

Note that v_s is the average solids velocity defined by

$$v_s = \frac{W_s}{\rho_b A} \tag{4}$$

The friction factor is a function of the design and operating parameters. In this study, since other parameters are held constant, the friction factor is expressed as

$$f_b = a_0 D_t^{a_1} \bar{d}_p^{a_2} U_g^{a_3} v_s^{a_4}. \tag{5}$$

The coefficients a_0 through a_4 are to be determined from experimental data.

Flow Curve

Analogous to the work of Metzner and Reed (1955), we define a wall shear stress as

$$\tau = \frac{D_t F_{w\tau}}{4AL} = \frac{D_t}{4}\left(\rho_b g \sin\theta - \frac{P_1 - P_2}{L}\right); \tag{6}$$

Table 1. Ranges of the Parameters

Parameter	Range
U_f, m/sec	0.35-1.00
h_b, m	0.045-0.197
h, m	0.35 and 0.68
L, m	0.44 and 0.62
P_c, N/m^2	$0\text{-}5.98 \times 10^3$
$\bar{d}_p$, m	5.1×10^{-4} and 2.9×10^{-4}
D_t, m	2.54×10^{-2} and 5.08×10^{-2}

an average shear rate as

$$\dot{\gamma} = \frac{8v_s}{D_t}, \tag{7}$$

and two coefficients n and k as

$$n = \frac{d \ln \tau}{d \ln \dot{\gamma}} \tag{8}$$

and

$$k = \frac{\tau}{\dot{\gamma}^n} \tag{9}$$

The coefficient n characterizes the degree of non-Newtonian behavior of all time-independent fluids. The greater the deviation of n from unity, the more non-Newtonian the fluid. The coefficient, k, defines the consistency of the fluid. The larger the value of k, the more viscous the fluid.

Metzner and Reed (1955) also proposed a generalized Reynolds number so that the conventional friction factor correlation for the flow of Newtonian fluids in pipes could be applied to a greater variety of time-independent non-Newtonian fluids. The generalized Reynolds number is defined as

$$Re_{MR} = \frac{D_t^n v_s^{2-n} \rho_b}{m}, \tag{10}$$

where

$$m = k \cdot 8^{n-1} \tag{11}$$

Thus, when the flow is in the laminar region, where $Re_{MR} < 2{,}100$, the following relationship holds

$$f_b = \frac{16}{Re_{MR}} \tag{12}$$

SETUP AND PROCEDURE

The experimental setup is schematically shown and discussed in Part I.

Three types of distributors were tested. Their geometric features are shown in Part I, Figures 2a, 2b, and 2c. During operation, the #7 distributor was oriented such that the half with the larger hole size was adjacent to the transfer line.

Based on the result of a preliminary investigation (Chen et al. 1978), the following operating and design parameters were selected for study (see Part I, Figure 1):

1) U_f, superficial fluidizing gas velocity;
2) h_b, height of the bottom of the transfer line relative to the distributor plate;
3) h, height of the overflow outlet relative to the distributor;
4) L, effective length of the transfer line;
5) P_c, pressure in the free board;
6) $\bar{d}_p$, harmonic mean particle diameter;
7) D_t, transfer line diameter.

The ranges of these parameters studied are listed in Table 1.

In the conduct of an experiment the air flow rate was regulated by valve V1. The free-board pressure, P_c, was set by adjusting valves V3 and V4. The pressure and the bed height were observed to ensure that steady state was reached. Valve V2 at the bottom of collector C3 was opened to clear any solids inside and then shut. At the moment valve V2 closed, a stop watch began to measure the solids overflow rate. After the timing started, but before the completion of solids discharge from column C2, the rate of gas leakage through the transfer line and the pressures at positions 1 through 6 were measured. In addition, we took readings of the rotameter, the temperature and the pressure gauges. Finally, when the solids level in C2 was about to reach the upper end of the transfer line, the air flow was suddenly terminated by shutting valve V2, and simultaneously the timing was terminated. The solids in C3 were emptied from the collector and weighed.

In addition to the overflow method described in the preceding paragraph, the tracer particle method was also used in some of the runs for measuring the rate of solids flow. Red tracer particles with a mean diameter of 0.0027 m were mixed in the sand. The mass ratio of the tracer particles to sand particles was maintained approximately at 1:60, to prevent the tracer from flowing through the transfer line in lumps. The time necessary for a tracer particle to pass between two points in the transfer line was recorded. We took as many readings as possible before the solids emptied in column C2.

Sand was used as the test material. The pertinent properties are summarized in Part I, Table 2.

FRICTION FACTOR CORRELATION

The experimental data were analyzed and are presented in terms of the friction factor correlation and the flow curves.

With the aid of a computer program for nonlinear parameter estimation (Bard 1967), the values of the parameters a_0 through a_4 in Equation (5) were determined by fitting the equation to the data obtained with distributor 10. This resulted in:

$$f_b = 1.314 \times 10^5 D_t^{0.7} \overline{d}_p^{1.655} U_g^{-0.663} v_s^{-1.553}. \quad (13)$$

Figure 2 compares the predicted results from Equation (13) with the experimental data transformed through Equation (3).

This result can be compared with that obtained from the data of Trees (1962), which give the following correlation (Chen et al. 1979)

$$f_b = 438 \cdot D_t^{0.7} v_s^{-1.78}. \quad (14)$$

The dependence of the friction factor on the pipe diameter, D_t, is essentially the same in both cases. The present correlation shows a significant influence of the gas velocity on the friction factor, while Equation (14) contains no gas velocity but still predicts the data well. An explanation for this is that the condition of flow in obtaining the data used to formulate Equation (14) is such that the gas leakage rate is almost constant. Nonetheless, the effect of gas velocity on the friction factor is consistent with what has been qualitatively reported by Trees (1962).

In addition to the back pressure, the pipe inclination, diameter, and length, he studied the dependence of solids flow on various types of pipe exit geometries with different

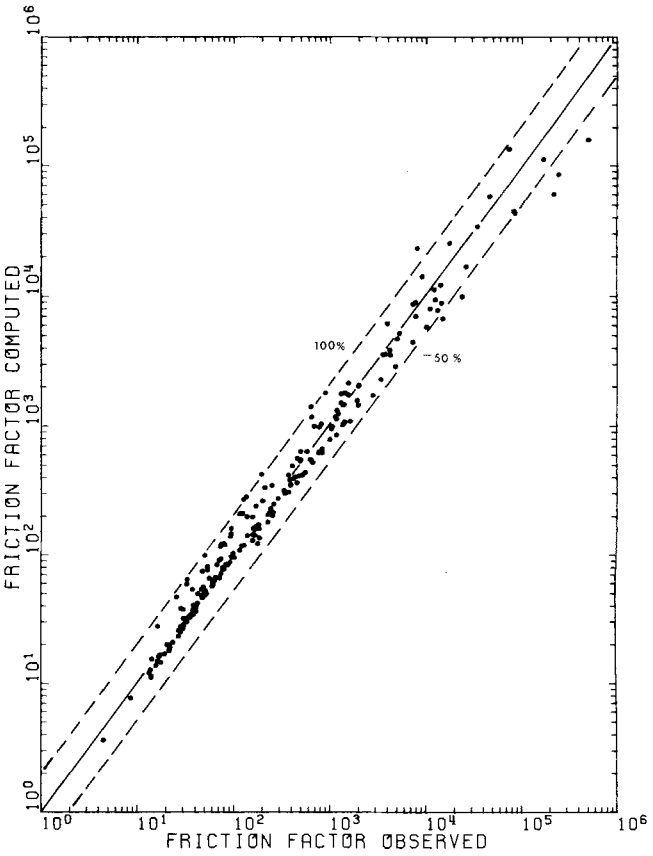

Figure 2. Comparison between the friction factor observed with distributor 10 and that computed from the correlation.

areas of projection onto the horizontal. He observed that an increase in the gas flow rate (resulting from an

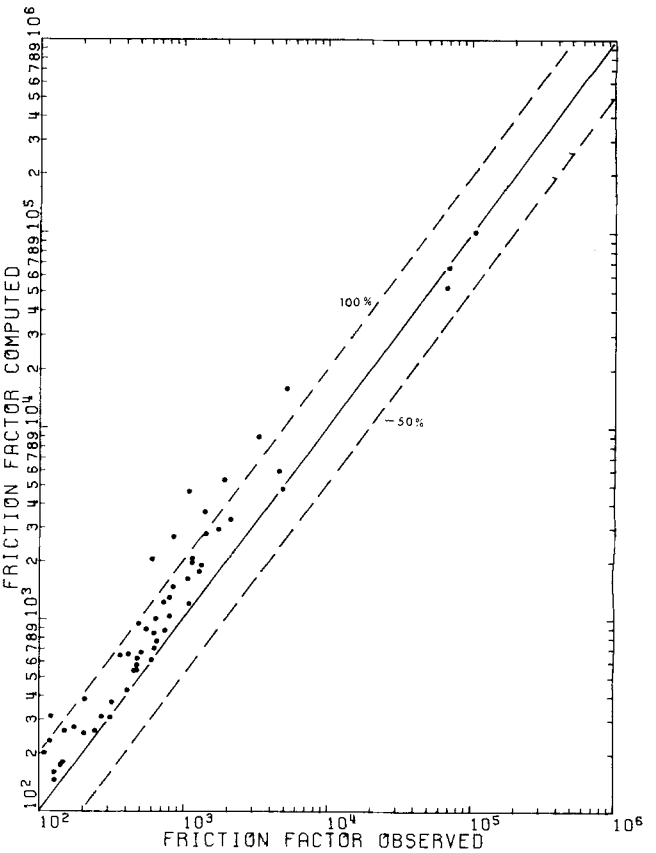

Figure 3. Comparison between the friction factor observed with distributor 7 and that computed from the correlation.

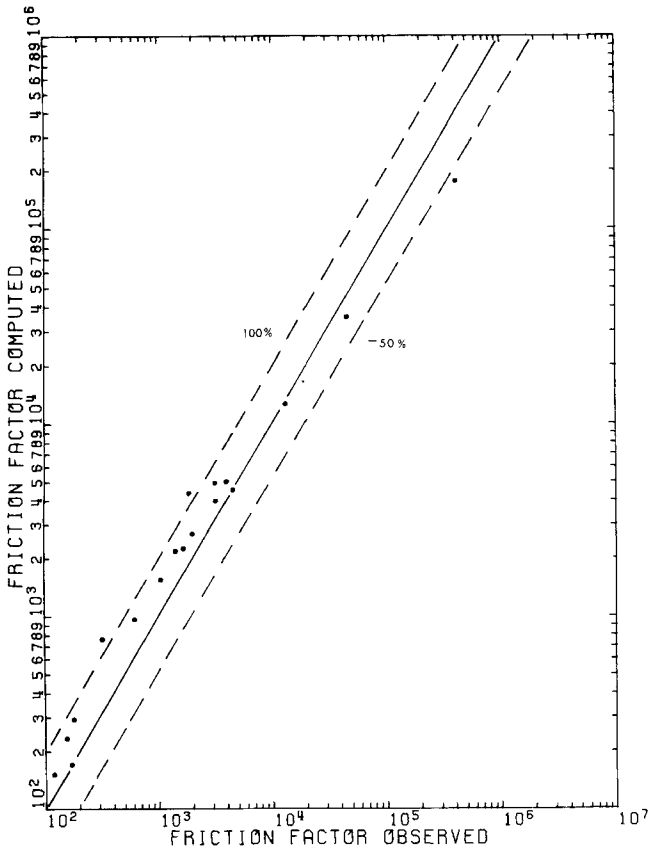

Figure 4. Comparison between the friction factor observed with distributor 1 and that computed from the correlation.

increased area of projection), gave rise to a faster solids flow—a smaller friction factor. The exponents of the solids velocity in the two correlations differ slightly from each other. This might be due to the difference in the design of the two flow systems. The exponent of the particle diameter in Equation (13) shows that it is easier for the smaller particles to flow. Equation (14) does not show the effect of particle diameter, because Trees used only one size of particle.

The predictions of the friction factor based on Equation (13) are compared with the data obtained with the other two distributors in Figures 3 and 4. Figure 3 shows that Equation (13) tends to overpredict the results obtained with distributor 7 (nonuniform). On the other hand, the predictions shown in Figure 4 for the results obtained with distributor 1 (uniform) are within the same

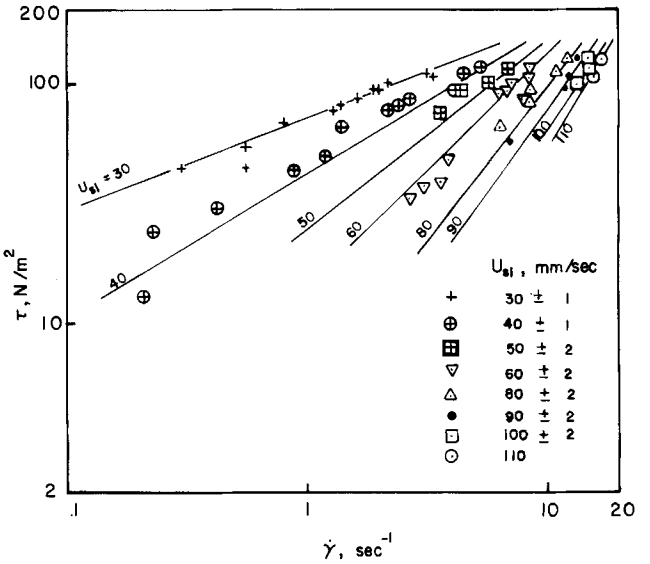

Figure 5. Typical plot of the shear stress vs. the average shear rate.

bounds of percentage error as those of Figure 2. This clearly reveals that a nonuniform distributor gives faster solids flow, while the hole area does not have significant effect on solids flow.

FLOW CURVE EQUATION

Figure 5 presents a typical plot of the wall shear stress, τ, against the average shear rate, $\dot{\gamma}$, with slip velocity as a parameter. The data in this figure were obtained with distributor 10, $D_t = 0.0508$ m, and $d_p = 0.00051$ m. The slip velocity is defined as

$$u_{sl} = U_g + \epsilon_g v_s \tag{15}$$

Note that, because of the countercurrent flow, a plus sign is used to define slip velocity. Data within the specified deviations from the same slip velocity are plotted with the same symbol. The following mechanistic model, as represented by the straight lines in the figure, has been fitted to the data.

$$\tau = k \dot{\gamma}^n \tag{16}$$

where

$$k = a_1 + \exp(a_2 - a_3 u_{sl}) \tag{17}$$

and

$$n = a_4 \{\exp[a_5(u_{sl} - a_7)] - \exp[a_6(u_{sl} - a_7)]\} \tag{18}$$

The parameters, a_1 through a_7, have been evaluated by

TABLE 2. RESULTS OF THE ESTIMATED PARAMETERS FOR FLOW CURVES

	Data set 1 Distributor 10	Data set 2 Distributor 7	Data set 3 Distributor 1
a_1	1.675	5.282×10^{-4}	8.524×10
a_2	8.174	6.522	7.275
a_3	5.380×10^{-1}	1.832	5.699×10^{-1}
a_4	2.931	1.246	3.144
a_5	-5.332×10^{-6}	-1.000×10^{-2}	-7.692×10^{-6}
a_6	-8.611×10^{-2}	-6.613×10^{-1}	-1.134×10^{-1}
a_7	1.374	1.472	1.410
Range of τ (N/m^2)	6.6-126	6.8-72.5	17.5-69.3
Standard deviation	7.91	8.59	6.74

$D_t = 0.0508$ m, $d_p = 0.000508$ m.

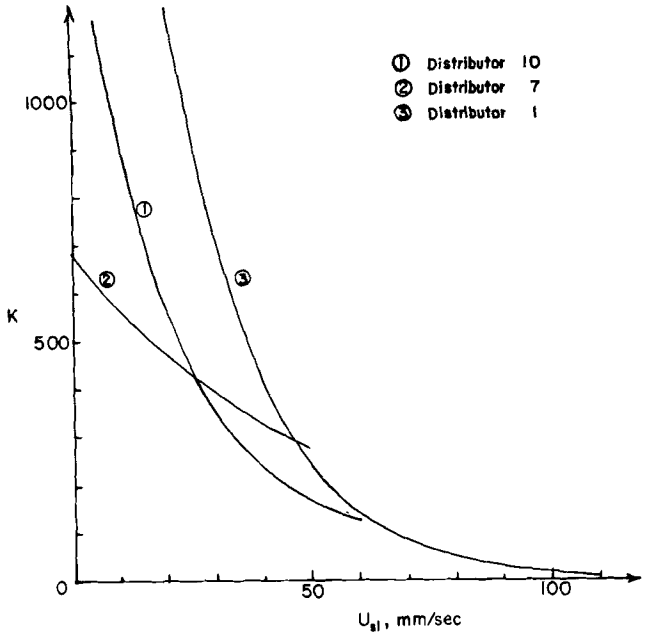

Figure 6. The variation of k with the slip velocity.

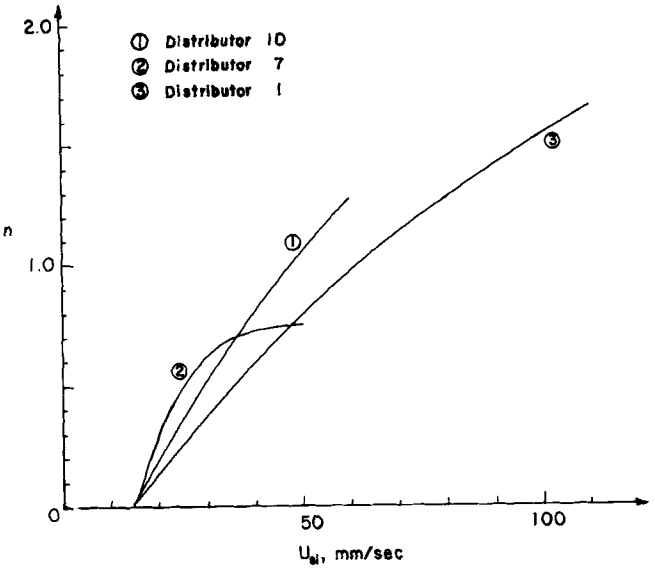

Figure 7. The variation of n with the slip velocity.

means of a nonlinear parameter estimation technique (Bard 1967), which minimizes the sum of squares of the difference between τ measured experimentally and that predicted by Equation (16). Values of these parameters, obtained with the three distributors, are presented in Table 2.

Figures 6 and 7 plot the best-fit values of k and n against the slip velocity. The numbers 1, 2 and 3 in the figures refer to the data set numbers in Table 2. Because too few experimental data were obtained with d_p = 0.00029 m and with D_t = 0.0254 m, these are not fitted to the model.

The common feature among the curves in Figure 6 is that k decreases as the slip velocity increases, indicating that the solids become less viscous and more fluid. The curves in Figure 7 show that there exists a critical velocity, u_0, below which n, the flow-behavior index, is negligibly small. In other words, at slip velocities below u_0, solids flow like a plug and, beyond u_0, a velocity profile starts to develop. This agrees with the observation that when the gas leakage rate was high, small gas bubbles flowed along the top layer in the transfer line and solids in different layers flowed at different velocities.

In either Figure 6 or 7, curve 2 is appreciably different from the others. The values of k for curve 2 in Figure 6

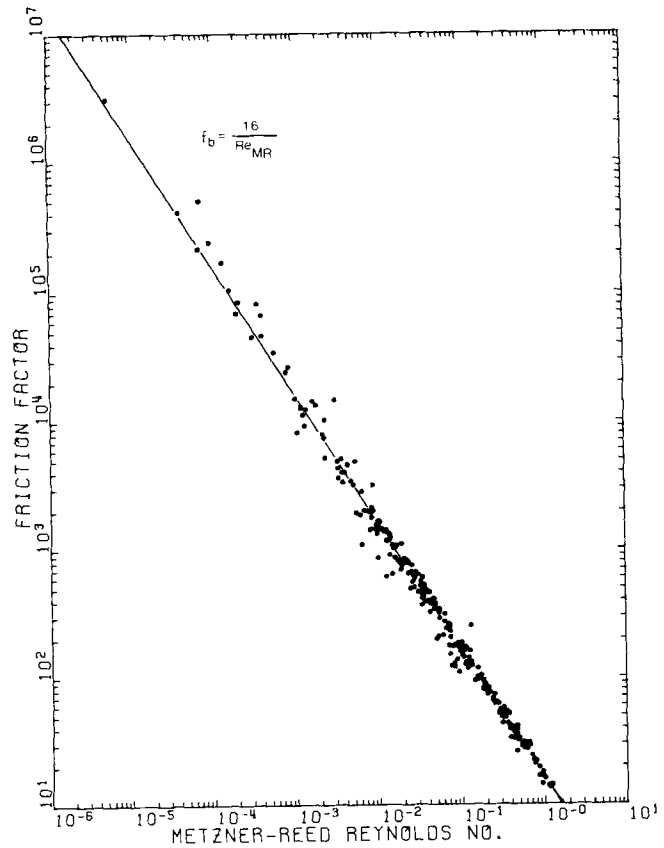

Fig. 8. Friction factor vs. the Metzner-Reed Reynolds number.

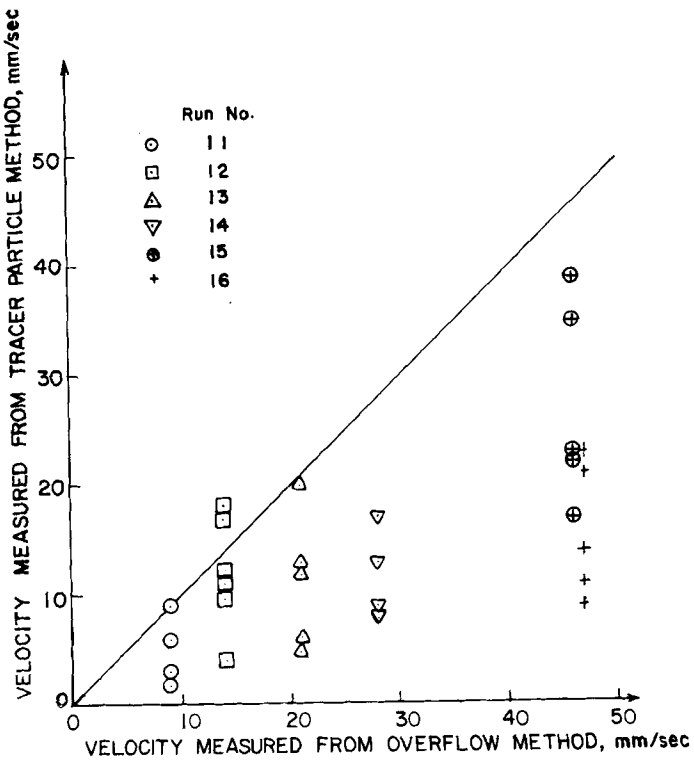

Fig. 9. Comparison between velocities measured from two different methods.

at negligibly small slip velocities are much smaller. The value of n for curve 2 in Figure 7 levels off to a lower value than for the others. This again shows the effect of using the non-uniform distributor on solids flow.

Figure 8 plots the friction factor, f_b, against the generalized Reynolds number of Metzner and Reed (1955), Re_{MR}, for different distributors. As expected, the data agree well with the prediction of Equation (12). By analogy, the flow can be considered laminar ($Re_{MR} < 2100$), meaning that the particles move in the pipe without significant change in their radial positions, as was observed.

METHODS FOR THE MEASUREMENT OF SOLIDS FLOW RATE

Figure 9 compares the velocities for the two methods of measurement. Different symbols are used to designate data from different runs. Because the solids flow under consideration is of the stick-slip type, the data obtained from the tracer-particle method fluctuate appreciably. They are, however, consistently lower than the results from the overflow method. Since the overflow method gives a bulk velocity while the tracer particle method measures the local velocity near the wall, results seem to suggest that the solids velocity in the center of the pipe is higher than that near the wall. This agrees with results of the preceding subsection, where the flow curves yield values of n greater than or equal to zero.

SOLIDS FLOW RATE ATTAINED

The maximum solids flow rate obtainable from the operating conditions used in this study was 0.336 kg/sec (2670 lb/hr) for the larger transfer line (0.0508 m I.D.). This value corresponds to a mass flux, that is the solids flow rate per unit cross-sectional area, of 165.5 kg/sec · m^2. (848 lb/hr. in.^{2}).

ACKNOWLEDGMENT

This is contribution No. 79-7j, Department of Chemical Engineering, Kansas Agricultural Experiment Station, KSU, Manhattan, Kansas 66506.

NOTATION

A = cross-sectional area of the transfer line
A_e = external surface area of the system
$\overline{dA}$ = an outwardly directed element of the external surface
D_t = diameter of the transfer line
d_p = harmonic mean particle diameter
F_i = external force per unit mass of the ith constituent of the system
F_{wr} = wall force due to friction
f_b = friction factor based on the solids bulk density
g = gravitational acceleration
h = fluidized bed height
k = consistency index
L = transfer line length
m = value defined by Equation (9)
n = flow behavior index
P = pressure
P_c = pressure in the freeboard
P_1 = pressure at the lower end of the transfer line
P_2 = pressure at the upper end of the transfer line
Re_{MR} = modified Reynolds number of Metzner and Reed defined by Equation (10)
t = time
$\overline{\overline{U}}$ = unit tensor
U_f = superficial fluidizing gas velocity
U_g = superficial gas velocity in the transfer line
U_{mf} = superficial velocity at minimum fluidization
u_0 = threshold velocity
u_{sl} = superficial slip velocity
V = volume
$\overline{u}$ = velocity vector
$\overline{v_e}$ = velocity vector of the external surface
v_s = solids velocity defined by Equation (4)
W_s = solids mass flow rate

Greek Letters

ϵ_g = volume fraction of the gas phase
$\dot{\gamma}$ = average shear rate
θ = angle of inclination from the horizontal
ρ = density
ρ_b = solids bulk density
ρ_g = gas density
ρ_i = density of the ith constituent of the system
τ = wall shear stress
$\overline{\overline{\tau}}$ = frictional stress tensor

LITERATURE CITED

Bailie, R. C., "Production of High Energy Fuel Gas from Municipal Wastes," U.S. Patent #3853498 (1974).

Bard, Y., "Nonlinear Parameter Estimation and Programming," IBM New York Scientific Center (December, 1967).

Bird, R. B., W. E. Stewart, E. N. Lightfoot, *Transport Phenomena* (Chapter 6), Wiley, New York (1960).

Chari, S. S., "Pressure Drop in Horizontal Dense Phase Conveying of Air-Solid Mixtures," *AIChE Symposium Series*, 67 (116), 77-84 (1971).

Chen, T. Y., W. P. Walawender, and L. T. Fan, "Transfer of Solids Between Parallel Fluidized Beds," *AIChE Symposium Series 176*, 74, 75-81 (1978).

Chen, T. Y., W. P. Walawender, and L. T. Fan, "Moving-Bed Solids Flow Between Two Fluidized Beds," *Powder Tech.*, 22, 89-96 (1979).

Engler, C. R., W. P. Walawender, and L. T. Fan, "Synthesis Gas from Feedlot Manure. Conceptual Design Study and Economic Analysis," *Environ. Sci. Technol.*, 13, 1152-1157 (1975).

Kunii, D., T. Kunugi, O. Yuzawa, and N. Kunii, "Flow Characteristics of Circulation Systems with Two Fluidized Beds," *Internat. Chem. Eng.*, 14, 588-593 (1974).

Kunii, D., M. Hasegawa, and J. Fukuda, "Research and Development of Circulation System Between Fluidized Beds for Application of Gas-Solid Reactions," Proceedings of Pachec '77, pp. 176-182 (1977).

Metzner, A. B., and J. C. Reed, "Flow of Non-Newtonian Fluids-Correlation of the Laminar, Transition, and Turbulent-flow Regions," *AIChE J.* (1), 434-440 (1955).

Standart, G., "The Mass, Momentum, and Energy Equation for Heterogeneous Flow Systems," *Chem. Eng. Sci.*, 19, 227-236 (1964).

Stemerding, S., "The Pneumatic Transport of Cracking Catalyst in Vertical Risers," *Chem. Eng. Sci.*, 17, 599-608 (1962).

Trees, J., "A Practical Investigation of the Flow of Particulate Solids through Sloping Pipes," *Trans. Instn. Chem. Eng.*, 40, 286-296 (1962).

Wilson, K. C., M. Streat, and R. A. Bantin, "Slip-Model Correlation of Dense Two-Phase Flow," Proceedings of the Second International Conference on the Hydraulic Transport of Solids in Pipes, 20th-22nd September (1972).

Manuscript received April 24, 1978; revision received June 12, 1979, and accepted July 6, 1979.